JACS
JOURNAL OF THE AMERICAN CHEMICAL SOCIETY

Communication

pubs.acs.org/JACS

Mechanical Properties of a Series of Macro- and Nanodimensional Organic Cocrystals Correlate with Atomic Polarizability

Thilini P. Rupasinghe, Kristin M. Hutchins, Bimali S. Bandaranayake, Suman Ghorai, Chandana Karunatilake, Dejan-Krešimir Bučar, Dale C. Swenson, Mark A. Arnold, Leonard R. MacGillivray,* and Alexei V. Tivanski*

Department of Chemistry, University of Iowa, Iowa City, Iowa 52242-1294, United States

Supporting Information

ABSTRACT: A correlation between Young's modulus, as determined by using nanoindentation atomic force microscopy (AFM), and atomic polarizability is observed for members of a series of cocrystals based on systematic changes to one cocrystal component. Time domain spectroscopy over terahertz frequencies (THz-TDS) is used for the first time to directly measure the polarizability of macro- and nanosized organic solids. Cocrystals of both macro- and nanodimensions with highly polarizable atoms result in softer solids and correspondingly higher polarizabilities.

Studies on the mechanical properties of organic crystalline solids have gained significant attention owing to potential applications in fields such as pharmaceutics, electronics, gas storage, biophysics, explosives, and device fabrication.[1−5] Mechanical property characterization is essential, for example, to achieve materials with increased tabletability in pharmaceutics and to understand structural changes (e.g., phase transitions).[6] For device fabrication, especially in flexible electronics, knowledge of mechanical properties is important to establish and optimize operational limits.[7] Understandings of mechanical properties can also provide insights into relative strengths of intermolecular interactions in solids (e.g., hydrogen bonds), which can serve to link size-dependent structural properties (e.g., elasticity) that span atomic to macroscopic levels.[8−10]

In this context, polarizability is a property of a chemical system that describes the tendency of charge distribution to be distorted in response to an external electric field. At the atomic level, polarizability increases as volume occupied by electrons increases, although much less is known regarding polarizabilities of molecules, assemblies of molecules, and those of corresponding bulk material solids. There is emerging evidence that polarizability can be *inversely* related to the stiffness of a material as measured by its Young's modulus.[11−15] Specifically, an inverse relationship between stiffness and atomic or molecular polarizability has been observed for metals, oxides, covalent crystals and polymers.[9,14−17] A linear relationship between molecular polarizability and compressibility, which is inversely proportional to Young's modulus, has been also demonstrated in halomethanes.[11] A linear relationship has also been noted between Young's modulus and binding energy within graphene nanoribbon materials, which was attributed to the decrease in molecular polarizability.[12,13] No such relationship has been discussed in the context of organic crystalline solids. Moreover, given that elastic properties of nanosized materials may differ considerably from larger and extended particles,[18] it will be of paramount importance to determine relationships between polarizability and mechanical properties to facilitate the rational design, or crystal engineering,[7,8] of novel multicomponent solids with controllable and useful physical-chemical properties.

Herein, we present Young's modulus and polarizability measurements on a series of macro- and nanodimensional organic cocrystals composed of either resorcinol (res) or 4,6-di-X-res (X = Cl, Br, I) and *trans*-1,2-bis(4-pyridyl)ethylene (4,4′-bpe) (Scheme 1). From atomic force microscopy (AFM) nanoindentation measurements,[18−23] we show that both macro- and nanosized cocrystals display a decrease in Young's modulus when the size of the substituent is increased from parent res (H) to Cl to Br to I. A correlation between the Young's modulus and polarizability is demonstrated through both measurements and DFT calculations. Terahertz (THz) time domain spectroscopy (TDS) is also used to directly measure the polarizabilities of the solids and, in doing so, verify the AFM measurements. Our work, thus, also establishes THz-TDS as a convenient and practical method to gain insight into relationships between atom-to-bulk properties of organic solids.

Scheme 1. Mechanical Properties of Cocrystals (Res)·(4,4′-bpe) and (4,6-di-X-Res)·(4,4′-bpe) (X = Cl, Br, I)

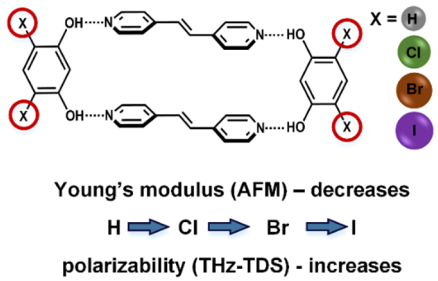

Our study involves macro- and nanosized cocrystals of (res)·(4,4′-bpe) **1**, (4,6-di-Cl-res)·(4,4′-bpe) **2**, (4,6-di-Br-res)·(4,4′-bpe) **3** and (4,6-di-I-res)·(4,4′-bpe) **4**. Macrosized crystals of **1** and **2** were generated as reported.[24,25] Macrosized crystals of **3** and **4** were formed via slow solvent evaporation of 4,4′-bpe and

Received: July 27, 2015
Published: September 25, 2015

DOI: 10.1021/jacs.5b07873
J. Am. Chem. Soc. 2015, 137, 12768−12771

the appropriate res (1:1 ratio) in EtOH. Formulations of **3** and **4** were confirmed using ^{1}H NMR spectroscopy and single-crystal X-ray diffraction. Nanosized cocrystals of **1**−**4** were readily generated using sonochemistry[12] (see Supporting Information, SI).

Single-crystal X-ray experiments reveal each solid to exhibit a closed hydrogen-bonded tetramer of molecules sustained by four O−H···N hydrogen bonds (O···N separations (Å): O(1)···N(1) 2.71(1), O(2)···N(2) 2.76(1) **3**; O(1)···N(1) 2.77(1), O(2)···N(2) 2.69(1) **4**) (Figure 1). Cocrystals **1**, **3**, and **4** are isostructural, crystallizing in the triclinic space group $P\bar{1}$, while **2** lies in the monoclinic space group $P2_1/n$.

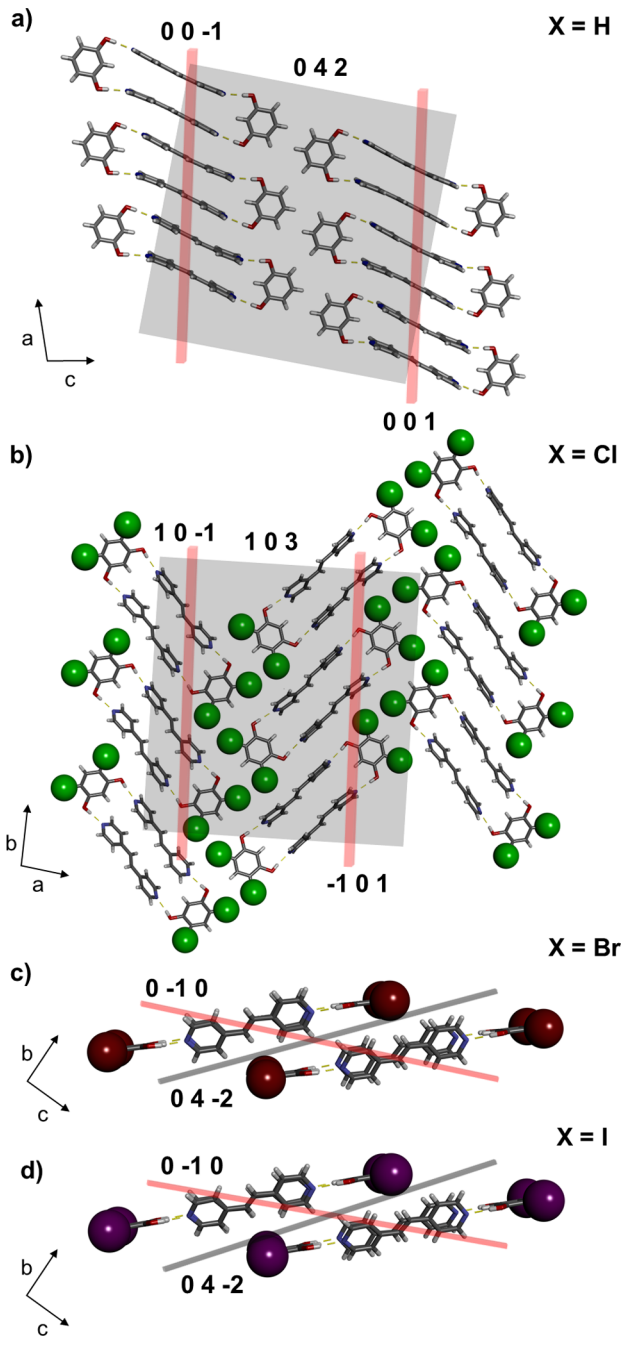

Figure 1. X-ray structures: (a) **1**, (b) **2**, (c) **3**, and (d) **4** highlighting layered packing of assemblies. AFM planes probed for macrosized crystals highlighted in red. Offset layers highlighted in gray.

The tetramers in each cocrystal self-assemble to form offset layers. The tetramers of **1** interact in the crystallographic (042) plane via face-to-face $\pi-\pi$ forces (C···C: 3.44 Å) of the olefins (Figure 1a). The layers stack offset along the *b*-axis and interact via C−H(pyridine)···O(res) (C···O: 3.33, 3.56 Å) and C−H(pyridine)···π(res) forces (C···C: 3.68 Å). Tetramers of **2** interact in the crystallographic (103) plane via Cl···Cl forces (3.55 Å). The Cl···Cl interactions are classified as Type II ($|\theta_1-\theta_2|$ = 36°),[26] which define halogen bonds between the res molecules (Figure 1b). The layers also stack along the *c*-axis via C−H(pyridine)···π(res) forces (C···C: 3.63 Å). For **3** and **4**, the tetramers interact in a layer via O···Br (3.16 Å, **3**) and O···I (3.22, **4**) forces, respectively (Figure 1c,d). While the O···Br and O···I distances are shorter than the van der Waals distances, the interactions are Type I ($|\theta_1-\theta_2|$ 2° (**3**) and 2° (**4**)), which is consistent with strong effects of close packing.[26−28] The layers stack offset, interacting via C−H(pyridine)···π(res) forces (C···C: 3.63 Å **3**, 3.61 Å **4**).

Characterizations of Young's moduli for both macro- and nanosized samples of **1**−**4** were carried out using AFM nanoindentation.[7,18] The macrosized cocrystals of **1**−**4** exhibited prism morphologies with bases ca. 0.30 × 0.05 mm and heights of ca. 0.05 mm. Top and bottom crystal faces that correspond to the crystallographic (001) and (00$\bar{1}$) planes of **1**, (10$\bar{1}$) and ($\bar{1}$01) planes of **2**, and (0$\bar{1}$0) and (010) planes for **3** and **4** were directly probed by AFM. The planes probed for **1** correspond to the long-axis of a hydrogen-bonded tetramer within a layer, extending along the *c*-axis (Figure 1a). The planes for **2** are also within a layer, extending along the *a*-axis (Figure 1b). The planes for **3** and **4** bisect neighboring layers that sit along the *b*-axis (Figure 1c,d).

Repeated force−displacement curves were recorded on the macrosized cocrystals at ca. 100 positions of both top and bottom faces. Top planes correspond to the initial phase of crystal growth, while bottom planes toward the end. Two conclusions are drawn from the histogram data of the Young's moduli measurements (Figure 2, left column and Table 1).[29] First, the top faces for **2**−**4** show 10−20% higher Young's modulus values relative to the bottom, while the Young's modulus for the top face of **1** is ∼20% lower than that for the bottom. The differences may reflect the presence of either hydrogen-bond-donor or -acceptor groups at the individual crystal surfaces (i.e., either res or 4,4′-bpe at face).[18,30] More importantly, the AFM measurements of the cocrystals show a general dependence of the Young's modulus on the nature of the res substituent (Figure 3a). Specifically, we observe an increase in crystal softness that is correlated with an increase in atomic polarizability[11] (H = 0.67, Cl = 2.18, Br = 3.05, I = 4.7 Å^3). The relationship is particularly noteworthy for isostructural **1**, **3**, and **4**, where the change across the series can be directly attributed to the identity of the H and halogen atoms.

We next studied nanosized cocrystals (bases ca. 0.8 × 0.8 μm and heights of ca. 50−200 nm) where the measurements are expected to yield an orientation averaged response and, thus, are considered more reflective of bulk properties[18] (Figure 2, Table 1). Specifically, similar to the macrosized solids, the nanodimensional cocrystals of **1** exhibited the highest Young's modulus values, followed by **2**, **3**, and **4**. Thus, a systematic decrease in Young's modulus was also observed with increasing atomic polarizability from H to Cl to Br to I (Figure 3a). The decrease in stiffness was on the order of 55% from H to Cl, 25% from Cl to Br, and 42% from Br to I. The nanosized X-substituted cocrystals also displayed a size-dependent increase in stiffness compared to the macrosized solids (33% for **2**, 120% for **3**, 95% for **4**).[11,18]

DOI: 10.1021/jacs.5b07873
J. Am. Chem. Soc. 2015, 137, 12768−12771

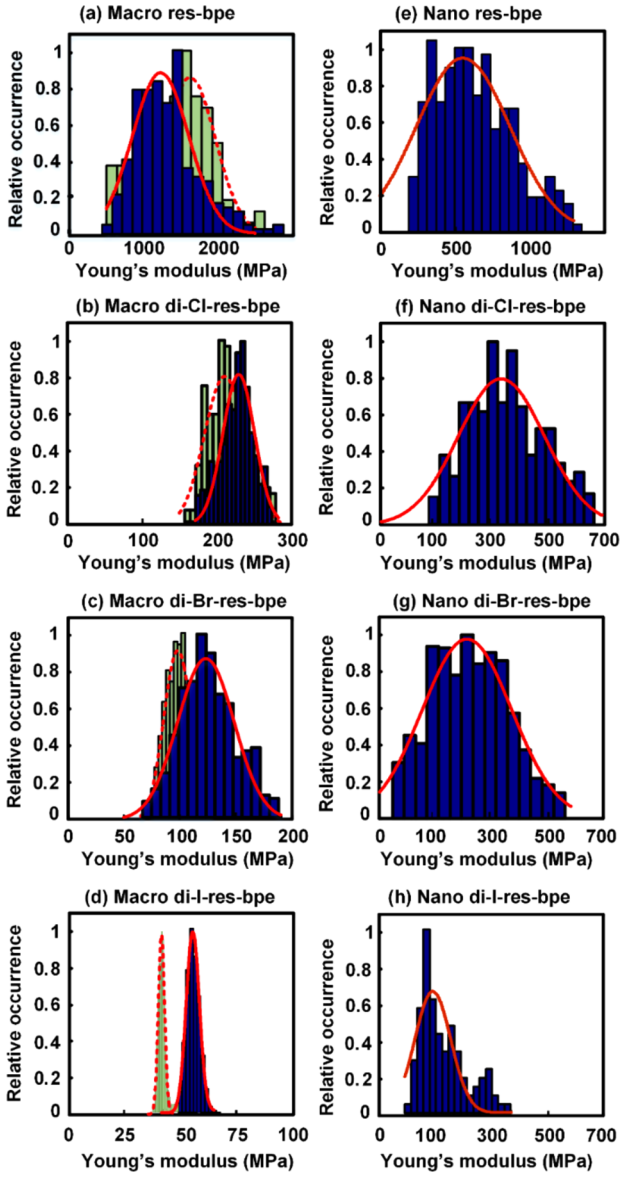

Figure 2. Histograms of Young's modulus for macro- (left) and nanosized (right) **1**−**4** (Gaussian fits as red lines). For macro crystals, top plane data in blue bars, bottom plane in green bars.

Table 1. Young's Modulus (YM) and Polarizability (α) Measurements[a]

sample	YM (MPa)	α (Å^3)
1-macro	1600 ± 350 (00−1)	88.5 ± 1.6
	1250 ± 350 (001)	
2-macro	270 ± 25 (10−1)	93.1 ± 0.7
	235 ± 25 (−101)	
3-macro	120 ± 15 (0−10)	98.3 ± 0.6
	95 ± 10 (010)	
4-macro	54 ± 3 (0−10)	104.1 ± 1.4
	40 ± 2 (010)	
1-nano	570 ± 200	87.6 ± 1.4
2-nano	370 ± 140	89.6 ± 1.0
3-nano	275 ± 140	97.5 ± 1.7
4-nano	160 ± 50	102.2 ± 1.3

[a]Crystallographic plane in parentheses.

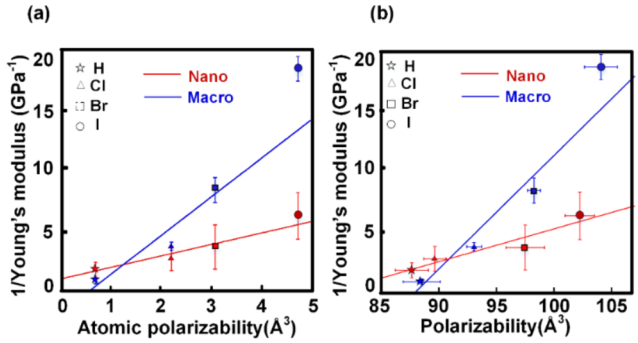

Figure 3. Plots: (a) inverse Young's modulus vs atomic polarizability for **1**−**4** (weighted fit macro R^2 = 0.85, nano R^2 = 0.93) and (b) inverse Young's modulus vs polarizability from THz-TDS for **1**−**4** (weighted fit macro R^2 = 0.93, nano R^2 = 0.93). Data for macrosized crystals for top plane (see SI for plot using bottom plane data).

To probe the observed correlation between Young's modulus and polarizability, we turned to THz-TDS. The coherent nature of THz spectroscopy permits a direct measure of polarizability as related to dielectric properties. THz-TDS is a rapidly developing technique that uses electromagnetic radiation (0.3−4.0 THz) to provide information related to vibrations in crystalline solids, intermolecular interactions in liquids, and rotational transitions in gases.[31−33] Dielectric constants were, thus, determined for **1**−**4** from 10 to 20 cm^{-1}. The constants were determined within 4−5 min by measuring the delay in a THz pulse transmitted across a pressed pellet composed of 5% cocrystal embedded within a matrix of polytetrafluoroethylene. Average values from measurements over several pellet preparations were used to calculate polarizability using the Clausius-Mossotti relationship (see SI).[34,35] Given the nature of the dielectric measurements, the resulting polarizability values correspond to ensemble measurements over a population of crystals randomly oriented with respect to the optical axis of the THz pulse, thereby, representing an average property of **1**−**4**.

In general, the measured polarizability values were comparable to benzoic acid, sucrose, and thymine as determined from THz-TDS measurements on single crystals (Figure 3 and Table 1).[36] Moreover, the polarizabilities from the THz-TDS measurements display a clear correlation (weighted fit macro R^2 = 0.93, nano R^2 = 0.93) with inverse Young's modulus obtained using AFM measurements (95% confidence limit) (Figure 3b). These results also agree qualitatively with DFT calculations using the RB3LYP method (see SI).[37,38] Hence, the polarizabilities of the solids increase with increasing size of the res substituent, which corresponds to the decrease in stiffness consistent with the expected inverse relationship.

While the correlation between Young's modulus and atomic polarizability in **1**−**4** may seem surprising given the highly anisotropic nature of organic crystals, two features of the crystal structures of **1**−**4** are noteworthy in relation to the mechanical data. First, the tetramers in each cocrystal assemble to form layers. That the components maintain layers across the series is likely a consequence of the isosteric relationship between the res derivatives. Atoms with comparable volumes are considered isosteric, while molecules that differ only in substitution of isosteres at a specific position are generally expected to form similar crystal structures.[39] Even the anomalous behavior of **2** in forming Type II halogen bonds[26,40] is unable to circumvent a tendency of the hydrogen-bonded tetramers to form a layered structure. The structural similarities of **1**−**4**, thus, allow the data

DOI: 10.1021/jacs.5b07873
J. Am. Chem. Soc. 2015, 137, 12768−12771

from the AFM measurements to be directly compared between the solids. Second, the interactions between the tetramers involve numerous weak and dispersive forces,[41] with the interactions involving the halogen atoms in **2**−**4** being considerably weak. Indeed, the O···X interactions in **3** and **4**, which are generally considered stronger than those of Cl···Cl forces in **2**,[27] fall within the definition of a weaker Type I halogen interaction wherein organization in the solid state arises owing to strong contributions of close packing.[26] Thus, in the absence of any particularly strong intertetramer forces[41] yet with layers pervading across the series, the general increase in softness and polarizability from **1** (H) to **4** (I) can be ascribed to the differences in atomic composition of the res components.

In this report, we have demonstrated that a bulk mechanical property in the form of Young's modulus for a series of organic cocrystals is correlated to atomic polarizability. The inverse relationship has been verified using THz-TDS, which establishes the analytical technique as a rapid and convenient method to obtain polarizability data related to atomic, molecular, and supramolecular structure. Given the now demonstrated relationship between chemical structure and physical properties, we expect present and future findings to establish atomic-to-bulk correlations that enable the rational design of a variety of multicomponent materials with desired mechanical and chemical properties.

Supplementary crystallographic data (CCDC 1025228, 1025229) can be obtained free of charge from the Cambridge Crystallographic Data Centre via www.ccdc.cam.ac.uk/conts/retrieving.html.

■ ASSOCIATED CONTENT

Supporting Information

The Supporting Information is available free of charge on the ACS Publications website at DOI: 10.1021/jacs.5b07873.

Experimental details, AFM height images of macro- and nanosized cocrystals, nanoindentation analysis, single-crystal and powder X-ray diffraction data, Terahertz spectra and theoretical calculations (PDF)
Crystallographic data for **3** and **4** (CIF)

■ AUTHOR INFORMATION

Corresponding Authors

*alexei-tivanski@uiowa.edu
*len-macgillivray@uiowa.edu

Notes

The authors declare no competing financial interest.

■ ACKNOWLEDGMENTS

T.P.R. and A.V.T. gratefully acknowledge financial support from the National Oceanic and Atmospheric Administration (NOAA) Climate Program Office, Earth System Science Program, award NA11OAR4310187. L.R.M. gratefully acknowledges partial financial support from the National Science Foundation (DMR-1408834).

■ REFERENCES

(1) Kosa, M.; Tan, J. C.; Merrill, C. A.; Krack, M.; Cheetham, A. K.; Parrinello, M. *ChemPhysChem* **2010**, *11*, 2332.
(2) Kim, T.; Zhu, L. Y.; Al-Kaysi, R. O.; Bardeen, C. J. *ChemPhysChem* **2014**, *15*, 400.
(3) Vogelsberg, C. S.; Garcia-Garibay, M. A. *Chem. Soc. Rev.* **2012**, *41*, 1892.
(4) Nath, N. K.; Panda, M. K.; Sahoo, S. C.; Naumov, P. *CrystEngComm* **2014**, *16*, 1850.
(5) Bolton, O.; Matzger, A. J. *Angew. Chem., Int. Ed.* **2011**, *50*, 8960.
(6) Mishra, M. K.; Varughese, S.; Ramamurty, U.; Desiraju, G. R. *J. Am. Chem. Soc.* **2013**, *135*, 8121.
(7) Reddy, C. M.; Krishna, G. R.; Ghosh, S. *CrystEngComm* **2010**, *12*, 2296.
(8) Varughese, S.; Kiran, M. S. R. N.; Ramamurty, U.; Desiraju, G. R. *Angew. Chem., Int. Ed.* **2013**, *52*, 2701.
(9) Hooks, D. E.; Ramos, K. J.; Bolme, C. A.; Cawkwell, M. J. *Propellants, Explos., Pyrotech.* **2015**, *40*, 333.
(10) Ramos, K. J.; Bahr, D. F. *J. Mater. Res.* **2007**, *22*, 2037.
(11) Donald, K. J. *J. Phys. Chem. A* **2006**, *110*, 2283.
(12) Zeinalipour-Yazdi, C. D.; Christofides, C. *J. Appl. Phys.* **2009**, *106*, 054318−1.
(13) Gilman, J. J. *Mater. Res. Innovations* **1997**, *1*, 71.
(14) Gilman, J. J. *Electronic Basis of the Strength of Materials*, 1st ed.; Cambridge University Press: New York, 2003.
(15) Gilman, J. J. *Chemistry and Physics of Mechanical Hardness*, 3rd ed.; Wiley: New York, 2009.
(16) Noorizadeh, S.; Parhizgar, M. *J. Mol. Struct.: THEOCHEM* **2005**, *725*, 23.
(17) Gilman, J. J. *AIP Conf. Proc.* **2006**, *845*, 855.
(18) Karunatilaka, C.; Bučar, D.-K.; Ditzler, L. R.; Friščić, T.; Swenson, D. C.; MacGillivray, L. R.; Tivanski, A. V. *Angew. Chem., Int. Ed.* **2011**, *50*, 8642.
(19) Ramamurty, U.; Jang, J. I. *CrystEngComm* **2014**, *16*, 12.
(20) Cook, R. F. *Science* **2010**, *328*, 183.
(21) Shulha, H.; Zhai, X. W.; Tsukruk, V. V. *Macromolecules* **2003**, *36*, 2825.
(22) Guo, S.; Akhremitchev, B. B. *Langmuir* **2008**, *24*, 880.
(23) Tranchida, D.; Kiflie, Z.; Acierno, S.; Piccarolo, S. *Meas. Sci. Technol.* **2009**, *20*, 095702.
(24) MacGillivray, L. R.; Reid, J. L.; Ripmeester, J. A. *J. Am. Chem. Soc.* **2000**, *122*, 7817.
(25) Sokolov, A. N.; Bučar, D.-K.; Baltrusaitis, J.; Gu, S. X.; MacGillivray, L. R. *Angew. Chem., Int. Ed.* **2010**, *49*, 4273.
(26) Mukherjee, A.; Tothadi, S.; Desiraju, G. R. *Acc. Chem. Res.* **2014**, *47*, 2514.
(27) Cao, D.; Hong, M.; Blackburn, A. K.; Liu, Z. C.; Holcroft, J. M.; Stoddart, J. F. *Chem. Sci.* **2014**, *5*, 4242.
(28) Mukherjee, A.; Desiraju, G. R. *IUCrJ* **2014**, *1*, 49.
(29) The determined values are comparable to similar cocrystals of (5-CN-res)·(4,4′-bpe) (260 MPa), protein crystals (165 MPa), and hyperbranched macromolecules (190 MPa).
(30) Bracco, G.; Acker, J.; Ward, M. D.; Scoles, G. *Langmuir* **2002**, *18*, 5551.
(31) Smith, R. M.; Arnold, M. A. *Appl. Spectrosc. Rev.* **2011**, *46*, 636.
(32) Zeitler, J. A.; Taday, P. F.; Pepper, M.; Rades, T. *J. Pharm. Sci.* **2007**, *96*, 2703.
(33) Nguyen, K. L.; Friščić, T.; Day, G. M.; Gladden, L. F.; Jones, W. *Nat. Mater.* **2007**, *6*, 206.
(34) Looyenga, H. *Physica* **1965**, *31*, 401.
(35) Naftaly, M.; Miles, R. E. *J. Appl. Phys.* **2007**, *102*, 043517.
(36) Jepsen, P. U.; Clark, S. J. *Chem. Phys. Lett.* **2007**, *442*, 275.
(37) Castro, R.; Berardi, M. J.; Cordova, E.; deOlza, M. O.; Kaifer, A. E.; Evanseck, J. D. *J. Am. Chem. Soc.* **1996**, *118*, 10257.
(38) Hinchliffe, A.; Perez, J. J.; Machado, H. J. S. *Electron. J. Theor. Chem.* **1997**, *2*, 325.
(39) Dikundwar, A. G.; Pete, U. D.; Zade, C. M.; Bendre, R. S.; Row, T. N. G. *Cryst. Growth Des.* **2012**, *12*, 4530.
(40) Type II interactions are less favored for Cl and we note that these interactions are relatively weak. The $|\theta_1-\theta_2|$ lies just above the 30° threashold.
(41) Ghosh, S.; Mishra, M. K.; Kadambi, S. B.; Ramamurty, U.; Desiraju, G. R. *Angew. Chem., Int. Ed.* **2015**, *54*, 2674.

DOI: 10.1021/jacs.5b07873
J. Am. Chem. Soc. 2015, 137, 12768−12771